Volume 17, Number 3, 2024. pp. 349-360

Jordan Journal of Physics

ARTICLE

An Investigation into Properties for $^{156}_{66}Dy$ Isotope Using IBM-1 and IVBM Model

Dalenda M. Nasef

Physics department, Faculty of Sciences, University of Tripoli, Libya.

Doi: **https://doi.org/10.47011/17.3.10**

Received on: 24/11/022; *Accepted on: 17/01/2023*

Abstract: The $^{156}_{66}Dy$ isotopes in the O (6) region were investigated. The positive ground-state band of $^{156}_{66}Dy$ nuclei was calculated using the interacting boson model (IBM-1) and the interacting vector boson model (IVBM). The negative parity band energies of the above isotope were calculated using (IVBM) only. We plotted the ratios $(\frac{E(I+2)}{E(2_1^+)}, \frac{E(I+2)}{E(I)}, r(\frac{(I+2)}{I}))$ and the E-GOS curve as a function of the spin (I) to investigate the properties of the yrast band. Accordingly, the best-fit values of the parameters were used to construct the Hamiltonian, and the electromagnetic transition probability B(E2) of this nucleus was determined. Theoretical energy levels of dysprosium-156 isotope with a neutron number N = 90 and spin parity up to 30_1^+ were obtained using the MATLAB-20 simulation program. A comparison of these calculated energy levels with the corresponding experimentally measured ones shows a good agreement. The results also draw our attention to the fact that the nucleus of interest deforms and exhibits gamma-instability properties.

Keywords: Dysprosium Isotopes, Even-even nuclei, Interacting Boson Model-1, Interacting Vector Boson Model, Negative parity, Yrast band.

Abbreviations and Acronyms, IBM: Interacting Boson Model, IVBM: Interacting Vector Boson Model, U(5): Spherical limit, SU(3): Axially deformed shape limit O(6): γ-unstable limit, SP(12; R): the non-compact symplectic group.

Introduction

Nuclear physics has generated a large amount of theoretical and experimental data related to the atomic nucleus. This wealth of information arises from numerous studies that attempt to penetrate the atomic nucleus, breaking it down into its various components. A critical task for nuclear physics researchers is to adopt one or more nuclear models, which serves as the first step in understanding observed and measured data, making connections, and drawing conclusions.

Despite the great success of many proposed nuclear models in combining data and "explaining nuclear properties", scientists have not yet reached a consensus on a definitive model, a unified comprehensive theory that can explain everything about nuclear composition and interactions [1].

The interacting boson model (IBM) is one of the outstanding approaches for describing the nuclear structure of medium-heavy nuclei with collective properties. Additionally, IBM was found to provide a phenomenological description of spectral data for a wide range of atomic nuclei exhibiting collective features, including those typically interpreted as anharmonic oscillators or deformed rotors [2]. IBM introduced a simple connection between IBM's parametric and geometric descriptions [3]. The states in IBM consist of s and d bosons with intrinsic momentums of 0 and 2, respectively [4]. The

Corresponding Author: Dalenda M. Nasef **Email:** d.nasef@uot.edu.ly

first and simplest version "of the interacting boson model" (IBM-1), described in Refs. [2, 5, 6], is based on some of the "concepts and fundamentals" used in earlier nuclear models. It characterizes nuclear properties using a fixed number of boson systems, with no distinction between proton bosons and neutron bosons [7, 8].

The interacting vector boson model (IVBM) [9-11] has proven to be suitable for an accurate description of the low-lying ground band of well-deformed even-even nuclei. It has been used to describe the negative parity band of the atomic nucleus as well, by considering the proton and the neutron bosons separately. The IVBM is fundamentally based on the algebra of the non-compact symplectic group SP(12; R), which serves as the dynamical symmetry group of the model. This algebra is based on the creation and annihilation operators for two types of vector bosons, called p and n bosons. These bosons differ in their pseudospin by ±1/2, within the three-dimensional oscillator potential. In the rotational limit of the IVBM, the reduction from the SP (12; R) to the So (3) angular momentum group is carried out by the compact unitary subgroup U(6) [12, 13]. The symplectic extension of the IVBM allows us to treat bands with positive and negative parity to be considered as yrast bands, meaning that the states with a given L minimize the energy value with respect to the number of bosons N to form the base state of the model [14]. For most deformed nuclei, the description of axisymmetric and reflection symmetric spheres is sufficient to reproduce the spectrum of the band [15].

The energy ratio $R_{4/2}$ of the first 4_1^+ and 2_1^+ excited states in an even-even nucleus, $R_{4/2} = \frac{E(4_1^+)}{E(2_1^+)}$, is often used as a good indicator that takes into account different collective motions of the nuclei and critical point symmetries, especially in the deep structure close to the core. It is known that, based on some ideal assumptions, the energy ratio is expected to be 10/3 for a well-deformed axisymmetric rotor, 2.5 for the gamma instability limit, and 2.0 for a spherical vibrator, corresponding to the dynamical symmetries SU(3), O(6), and U(5), respectively. These symmetries degenerate from the group U(6), which governs the most general two-body Hamiltonian within the boson space among bosons [16-20].

Furthermore, the E-GOS curve (E-gama over spin) is a good tool for classifying nuclei. The E-GOS curve can actually follow the expected trend [17, 21].

Various nuclear observations have indicated multiple types of deformations after measuring certain multipole moments. Numerous signs of nuclear shape phase transitions were also observed [22]. For some isotopes, there is a shape transition from vibration to axial rotation or gamma-labile rotation associated with neutron number changes [23]. A type of collective movement can involve different characteristics. For example, along the yrast line transitions between rotations can occur, with a different relationship between angular momentum and rotational frequency, which is called a band crossing (with back-bending) [24, 25]. To correctly describe phenomena like the moment of inertia and back-bending frequency, it is important to consider not just pairs of monopoles but also pairs of double-stretched quadrupoles, despite their minimal impact on energy [20, 26].

In this research, the dysprosium-(156) isotope with atomic number Z = 66 was studied theoretically using the IBM-1 and the IVBM modules. While the IBM-1 model and IVBM modules were used to calculate the energy of the positive ground state band of the $^{156}_{66}Dy$ nucleus, the negative parity band energies of $^{156}_{66}Dy$ were calculated using the IVBM model only [17].

Theoretical Description

1) **IBM-1 Model:**

In the interacting boson model-1, the low-energy collective property of even nuclei can be generated as the state of N bosons. Namely, there is no difference in the degrees of freedom of the proton and neutron bosons. The N bosons are integrated by introducing six boson degrees of freedom and occupy two levels: one with angular momentum L = 0, called the s bosons, and the other a quadrupole boson with angular momentum L = 2, called the d boson [27, 28]. Furthermore, the model assumes that the structure of the low-lying band is determined by the excitations between valence particles outside the closed main shell [29].

The underlying structure of the model's six-dimensional unitary group U(6) leads to a simple Hamiltonian capable of describing the

three dynamical symmetries U(5), SU(3), and O(6) [30, 31]. The most general IBM Hamiltonian can be expressed as [32, 33]:

$$H = \sum_{i=1}^{N} \varepsilon_i + \sum_{i<j}^{N} V_{ij} \quad (1)$$

where ε_i is the fundamental boson energy and V_{ij} is the potential interaction between bosons i and j [34].

The Hamiltonian, in its multipole form, is written as [35]:

$$\hat{H} = \varepsilon \hat{n}_d + \alpha_o \hat{P}\hat{P} + \alpha_1 \hat{L}\hat{L} + \alpha_2 \hat{Q}\hat{Q} + \alpha_3 \hat{T}_3 \hat{T}_3 + \alpha_4 \hat{T}_4 \hat{T}_4 \quad (2)$$

where $n_d = (d^{\dagger}.d)$ is the total number of d boson operators, P = 1/2[(d.d) – (s.s)] is the pairing operator, $L = \sqrt{10}[d^{\dagger} \times d]^{l}$ is the angular momentum operator, and Q is the quadrupole operator, defined as:

$$Q = [d^{\dagger} \times s \times s^{\dagger} \times d]^{(2)} + \chi[d^{\dagger} \times d]^{(2)}.$$

Here, (χ) is the quadrupole structure parameter, with values of 0 and $\pm\sqrt{7}/2$.

In Eq. (2), Tr represents the octupole (r = 3) and hexadecapole (r = 4) operators, while $\varepsilon = \varepsilon_d - \varepsilon_s$ is the intrinsic boson energy [33, 35]. The parameters $\alpha_o, \alpha_1, \alpha_2, \alpha_3, and\ \alpha_4$ represent the pairing strength, angular momentum, quadrupole, octupole, and hexadecapole interactions between bosons, respectively. The Hamiltonian can be rewritten in terms of the Casimir operator of the U(6) group, in which case the Hamiltonian H can be said to have dynamical symmetries; these symmetries are called the SU(5) vibrational symmetry, SU(3) rotational symmetry, and O(6) γ-unstable symmetry [36].

The eigenvalues of O(6) dynamic symmetry can be written as [2]:

$$E = K_3(N - \sigma)(N + \sigma + 4) + K_4\tau(\tau + 3) + K_5 L(L + 1) \quad (3)$$

where $K_3 = \alpha_o/4$, $K_4 = \alpha_3/2$, $K_5 = \alpha_1 - \alpha_3/10$. $N = N_{\pi} + N_{\nu}$ with N representing the absolute number of bosons, N_{π} the number of valence protons relative to the nearest closed shell, and N_{ν} the corresponding number of valence neutrons. The variable σ = N, N−2, ..., 0 or 1, but for the low energy-momentum band we can set σ = N.

O(6) is marked with quantum numbers τ = σ, σ−1, ..., 0; L = 2λ, 2λ −2, ..., λ +1, where λ is a non-positive integer defined as λ = τ−3υ_, υ_ = 0, 1, and υ_ is the number of triplet bosons. σ is O(6) non-reducible representations, while τ is the O(5) [37, 38]. The preceding equation starts out as follows;

$$E = K_4\tau(\tau + 3) + K_5 L(L + 1) \quad (4)$$

2) **E-GOS:**

E-GOS (E-gama over spin) is one of the most important methods for determining the properties of the nuclei at different energy states, and it can be done by plotting the relationship between the gamma energy (E_{γ}) divided by the spin (I) as a function of the spin (I). This relationship for the three limits (vibrational, rotational and γ-unstable) is given as follows [39]:

$$U(5): R = \frac{\hbar\omega}{I} \xrightarrow{I\to\infty} 0 \quad (5)$$

$$SU(3): R = \left(\frac{\hbar^2}{2J}\right)\left(4 - \frac{2}{I}\right) \xrightarrow{I\to\infty} 4\left(\frac{\hbar^2}{2J}\right) \quad (6)$$

$$O(6): R = \frac{E(2_1^+)}{4}\left(1 + \frac{2}{I}\right) \xrightarrow{I\to\infty} \frac{E(2_1^+)}{4} \quad (7)$$

3) **Back-bending:**

To determine if the isotope has got back-bending property and to identify the location of the back-bending if it was found, we should examine the relationship between the moment of inertia ($2J/\hbar^2$) and gamma energy (E_{γ}). This relationship can be written as [8, 39]:

$$2J/\hbar^2 = \frac{4I-2}{E_{\gamma}} \quad (8)$$

While the relation between the ħω and E_{γ} is given by [40]:

$$\hbar\omega = \frac{E_{\gamma}}{\sqrt{I(I+1)} - \sqrt{(I-2)(I-1)}} \quad (9)$$

4) **B(E2) Values:**

A successful nuclear model must be able to accurately describe the energy spectrum of the nucleus and its electromagnetic properties. This property provides a good test of the nuclear structure and the wave function of the nuclear model [37, 41]. The reduction probability of the electric quadrupole transition B(E2) depends on the available experimental data on the half-lives of quantum transitions between energy levels. This probability is given by the relationship:

$$B(E2) = \frac{0.05657}{T_{\frac{1}{2}}^{Y}(ps)E_{\gamma}^{5}(MeV)}(e^2b^2) \quad (10)$$

In the case of just one transition out of the level, the relationship is:

$$T_{\frac{1}{2}}^{\gamma} = T_{\frac{1}{2}}(\exp)(1 + \propto_{tot}) \quad (11)$$

where $\propto_{tot}$ is the internal transformation coefficient [42].

5) **IVBM Model:**

The scientists extended the IVBM by incorporating its symplectic dynamical symmetry Sp(12, R), which makes it possible to vary the number of bosons representing blockages in the Hamiltonian model. This symplectic extension of the interacting vector boson model enables a more comprehensive classification of states than the single version and provides more opportunities to consider other collective bands [43].

Nuclear states are considered as a system of an even number of p-bosons with isospin T = 1/2 in the interacting vector boson model. This model is somewhat similar to the interacting boson model. For example, both models have solvable dynamic symmetries SU(3). By assigning angular momentum L and isospin T (LT = 01, 21, 10) for each boson pair in the ideal space of S, D bosons (T = 1) and P bosons (T = 0), we can find the relationship between the two models. We use the results that we can get by applying the dynamical symmetry algebra of IVBM, which is the non-compact symplectic algebra Sp(12, R), for the boson mapping[43-45].

The permissible values of energy states of the two bands, GSB and NPB, are given in the IVBM model by [43, 46]:

$$E(I)_{GSB} = \beta I(I+1) + \gamma I \quad (12)$$

and

$$E(I)_{NPB} = \beta I(I+1) + (\gamma + \eta)I + \zeta \quad (13)$$

Here, the parameter β represents the intensity of the effect of the rotational properties, while γ represents the intensity of the effect of the vibrational properties on the nucleus. The parameters η and ζ are crucial for determining the values of the energy states in the NPB beam. The values of these parameters can be determined by matching the experimental values of the energy states with Eqs. (1) and (2).

The GSB and NPB bands, with their distinct states $I^{\pi} = 0^+, 2^+, 4^+, \ldots \; and \; I^{\pi} = 1^+, 3^+, 5^+, \ldots$, respectively, overlap to form a single band called the octupole band $I^{\pi} = 0^+, 1^-, 2^+, 3^-, 4^+, 5^-, \ldots$. This overlap is a good example of the staggering of energies between these two bands, caused by the fact that an energy level of I exchanges its location with an energy level of I+1 [47]. The relationship of the staggering of patterns between the two bands is given as:

$$\Delta E_{1,\gamma}(I) = \frac{1}{16}\Big(6E_{1,\gamma}(I) - 4E_{1,\gamma}(I-1) - 4E_{1,\gamma}(I+1) + E_{1,\gamma}(I-2) + E_{1,\gamma}(I+2)\Big) \quad (14)$$

and

$$E_{1,\gamma}(I) = E(I+1) - E(I) \quad (15)$$

The ratio between any two consecutive states in the beam is important for determining state properties for the even-even nucleus and is given by:

$$r\left(\frac{(I+2)}{I}\right) = \left(R\left(\frac{I+2}{I}\right)_{exp} - \frac{(I+2)}{I}\right) \times \frac{I(I+1)}{2(I+2)} \quad (16)$$

Here, $R\left(\frac{I+2}{I}\right)_{exp}$ represents the ratio between experimental states I+2 and I. If the ratio $r\left(\frac{(I+2)}{I}\right)$ falls between 0.1 and 0.35, the nuclei have vibrational properties; if it is between 0.4 and 0.6, the nuclei have $\gamma - unstable$ properties; and if it is between 0.6 and 1.0, the nuclei have rotational properties.

Results and Discussion

The investigation of the nuclear structure and its deformation of the dysprosium isotope (156) was conducted using the IBM-1 and IVBM models. Dysprosium isotope (156) has an atomic number Z = 66, so it has eight proton bosons (middle shell) and four neutron bosons, so the total number of bosons for this isotope is 12. Eq. (4) is used to calculate the values of the parameters K_4 and K_5 twice, once for the baseband and once for the s-band, and Table 1 shows these values along with the number of isotopic bosons.

TABLE 1. Number of bosons and IBM-1 parameters of g and s bands in KeV.

isotope	N_π	N_ν	Total # of Bosons	g-band		s-band	
				K_4	K_5	K_4	K_5
$^{156}_{66}Dy$	8	4	12	24.023	6.9464	91.787	-17.12

By simulating the IBM-1 eigenvalue Eq. (4) using the MATLAB-20 program, we obtained the energy levels of the positive Yrast band. Furthermore, we also calculated the energy levels of the negative parity bands using Eqs. (12) and (13) obtained from the IVBM. Table 3 shows that the results are very close to the experimental data, and the IBM-1 model gives more accurate results than the positive parity band of the IVBM model, as shown in Fig. 1.

TABLE 2. IVBM parameters of GSB and NPB in KeV.

Isotop	β	γ	η	ζ
$^{156}_{66}Dy$	9.7	39.9	-38.8	1272.7

TABLE 3. Positive and negative energy levels for $^{156}_{66}Dy$.

Spin (I^π)	E_{exp} *(KeV)*	E_{clc} *(KeV)*	*Error (%)*
0^+	*0*	*0*	*0*
1^-	*1293.2*	*1293.2*	*0*
2^+	*137.77*	*137.8*	*0*
3^-	*1368.4*	*1392.3*	*-1.75*
4^+	*404.19*	*379.2*	*6.19*
5^-	*1526.3*	*1569.0*	*-2.80*
6^+	*770.44*	*724.2*	*6.01*
7^-	*1810*	*1823.3*	*-0.74*
8^+	*1215.61*	*1172.8*	*3.52*
9^-	*2186.6*	*2155.2*	*1.43*
10^+	*1725.02*	*1725*	*0.0*
11^-	*2636.6*	*2564.8*	*2.72*
12^+	*2285.88*	*2285.9*	*0.0*
13^-	*3154.2*	*3051.9*	*3.24*
14^+	*2887.82*	*2830*	*2.00*
15^-	*3719.6*	*3616.6*	*2.77*
16^+	*3523.3*	*3420.8*	*2.90*
17^-	*4331.1*	*4258.9*	*1.67*
18^+	*4178.1*	*4058.2*	*2.87*
19^-	*4978.8*	*4978.8*	*0.0*
20^+	*4859*	*4742.2*	*2.40*
21^-	-	-	-
22^+	*5573*	*5472.8*	*1.80*
23^-	-	-	-
24^+	*6328.7*	*6250*	*1.24*
25^-	-	-	-
26^+	*7130.3*	*7073.9*	*0.79*
27^-	-	-	-
28^+	*7978.5*	*7944.4*	*0.43*
29^-	-	-	-
30^+	*8875.9*	*8861.5*	*0.16*
31^-	-	-	-
32^+	*9825.2*	*9825.2*	*0.0*

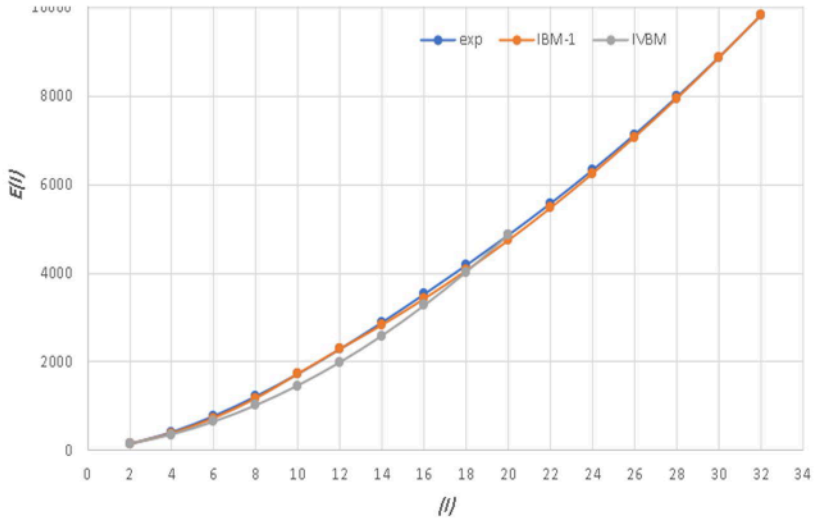

FIG. 1. Theoretical and practical energy levels as a function of angular momentum.

By examining the 2_1^+ energy level value for the $^{156}_{66}Dy$ isotope, we found that it to be approximately 137.8 KeV. This led us to expect rotational symmetry of the isotope, but when we performed other tests, we found dissimilarity! To determine the symmetry of the Dy(156) isotope, we calculated the energy ratios ($\frac{E(I+2)}{E(2_1^+)}$. The result aligned with the γ-unstable symmetry, as the typical ratios for γ-unstable O(6) were closest to the calculated values [1, 5]. Table 4 compares the calculated ratios using the IBM-1 with experimental ratios. Table 5 provides the typical values of the ratios to compare them with the calculated values and determine the type of symmetry that appeared to be O(6), see Fig. 2.

TABLE 4. Comparison of practical and theoretical energy ratios.

Isotope	$E(4_1^+)/E(2_1^+)$		$E(6_1^+)/E(2_1^+)$		$E(8_1^+)/E(2_1^+)$		$E(10_1^+)/E(2_1^+)$	
	EXP	IBM-1	EXP	IBM-1	EXP	IBM-1	EXP	IBM-1
$^{156}_{66}Dy$	2.93	2.75	5.59	5.26	8.82	8.51	13.5	12.52

TABLE 5. Typical values for energy ratios.

Symmetry	$E(2_1^+)$	$E(4_1^+)/E(2_1^+)$	$\frac{R_6}{2}$	$\frac{R_8}{2}$	$\frac{R_{10}}{2}$
U(5)	500	$2 \leq \frac{R_4}{2} \leq 2.4$	3	4	5
O(6)	300	$2.4 \leq \frac{R_4}{2} \leq 2.7$	4.5	7	10
SU(3)	100	$3 \leq \frac{R_4}{2} \leq 3.3$	7	12	18.33

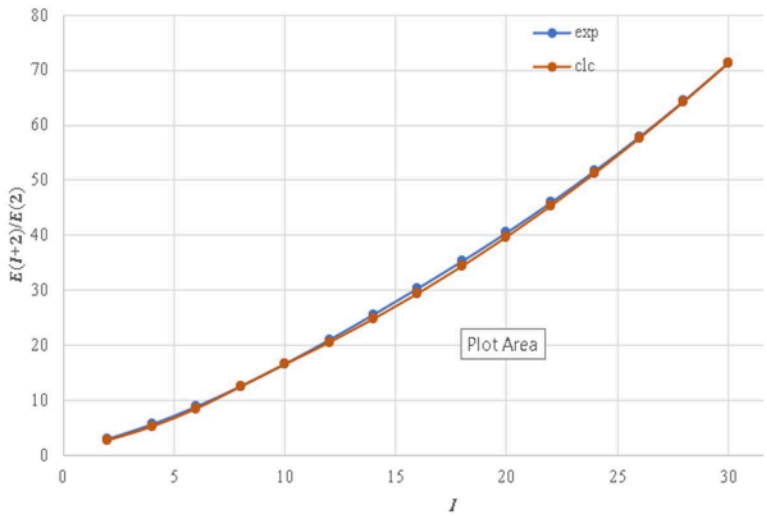

FIG. 2. Ratios with respect to the first energy level (2_1^+)

In addition, the ratios $\frac{E(I+2)}{E(I)}$ were calculated and compared with the typical values (Table 6 and Fig. 3), where the results showed that the Dy-156 isotope is closer to following the O(6) limit. Moreover, we have determined the symmetry using the E-GOS method and we have made sure that the isotope has γ-unstable symmetry (Fig. 4).

TABLE 6. Comparison between typical and calculated values for energy ratios.

symmetry	$R_{4/2} = E(4_1^+)/E(2_1^+)$	$R_{\frac{6}{4}}$	$R_{\frac{8}{6}}$	$R_{\frac{10}{8}}$	$R_{\frac{12}{10}}$
U(5)	2	1.5	1.33	1.25	1.2
O(6)	2.5	1.8	1.56	1.43	1.35
SU(3)	3.33	2.1	1.71	1.53	1.42
$^{156}_{66}Dy$ EXP	2.93	1.90	1.58	1.42	1.33
$^{156}_{66}Dy$ CLC	2.75	1.91	1.62	1.47	1.33

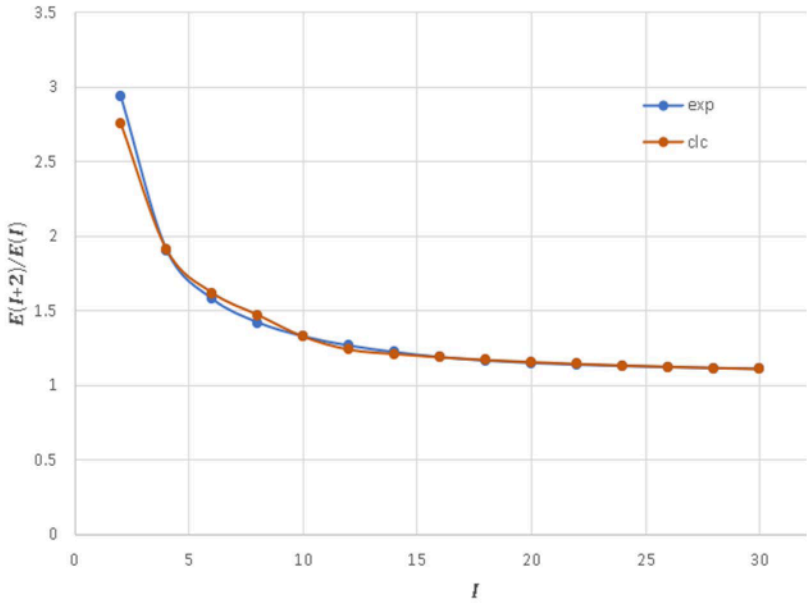

FIG. 3. Ratios with respect to variable states.

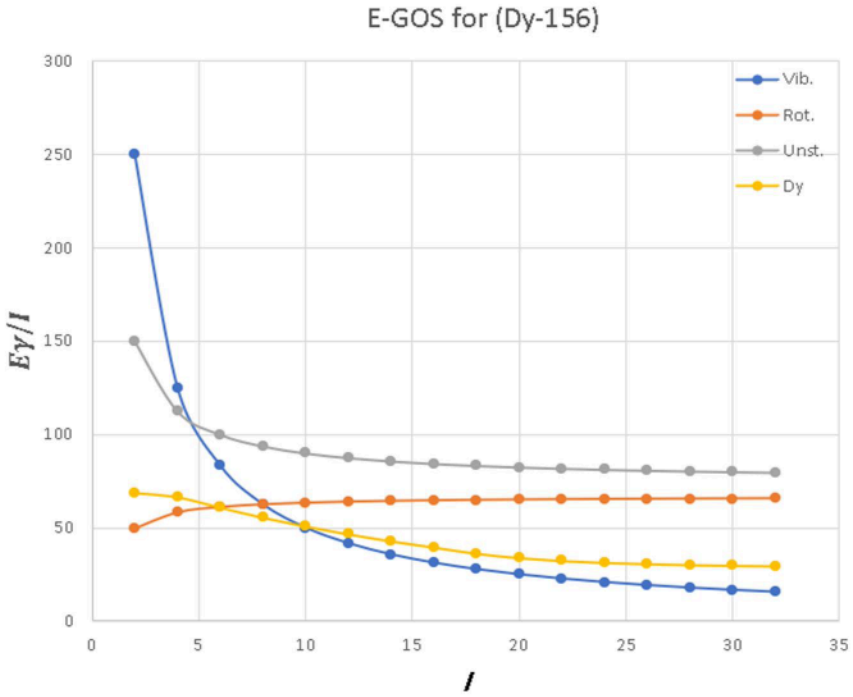

FIG. 4. E-GOS for $^{156}_{66}Dy$.

To determine the presence and location of back-bending in this isotope, the moment of inertia was calculated using Eq. (8), along with the transition energy E_γ between consecutive energy levels. The rotational frequency $\hbar\omega$ for each even spin was also calculated using Eq. (9). Fig. 5 shows the relationship between the moment of inertia and the rotational frequency for the isotope under study. Unbending rather than back-bending was observed due to the strong interaction between the ground-state band and the spin-aligned S-band [48, 49]. However, there was a difference in the isotope behavior at angular momentum in the range of 10-20 compared to the ranges of 0-10 and 20-30.

The energy of each level was plotted as a function of the angular momentum J(J+1) in Fig. 6, to check what we had found in the previous figure. In order to know more about the nature of the back-bending, we plotted E_γ as a function of J in Fig. 7. This plot shows that there is a continuous increase without a decrease in the transmission energy with an increase in momentum, and this confirms the observations from the last two figures.

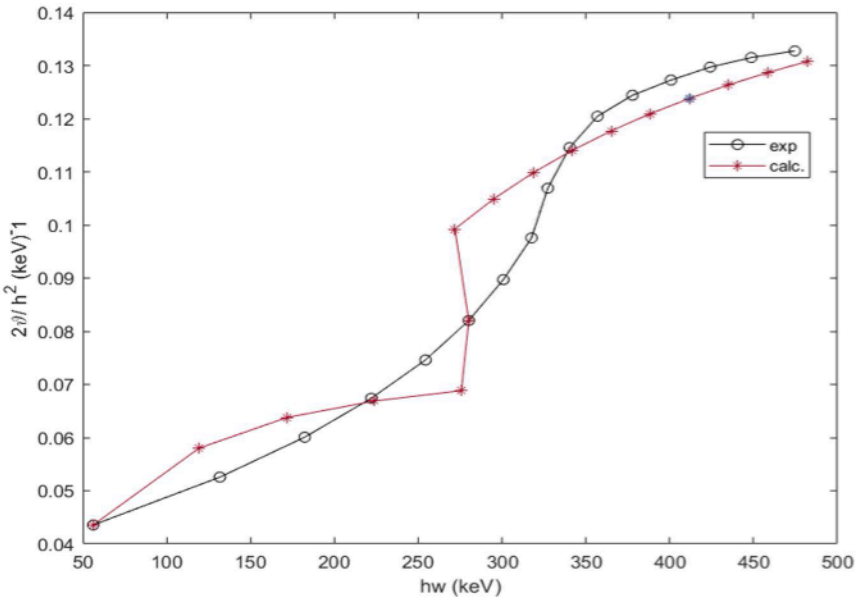

FIG. 5. Back-bending phenomena.

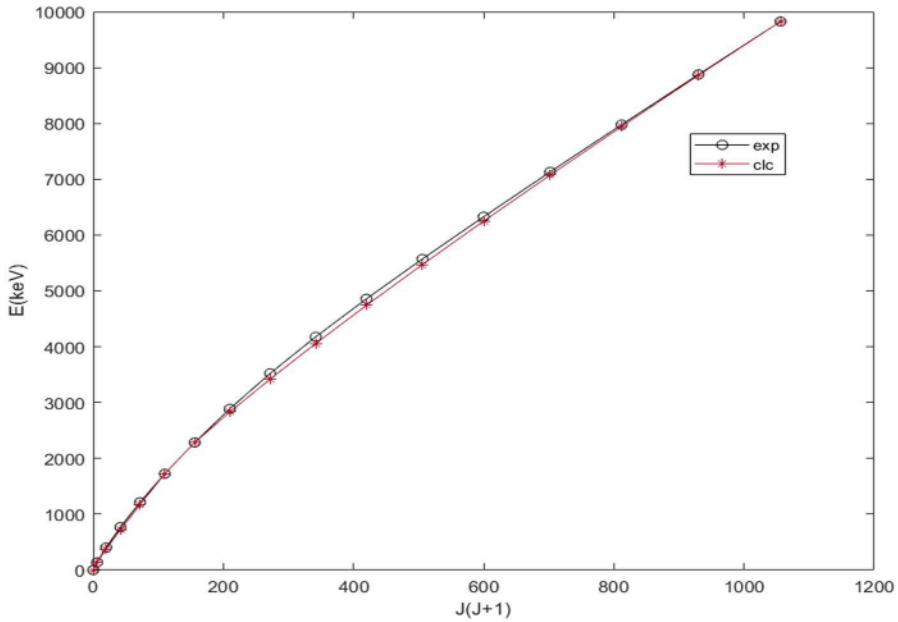

FIG. 6. Experimental and IBM-1 calculated energy levels as a function of spin.

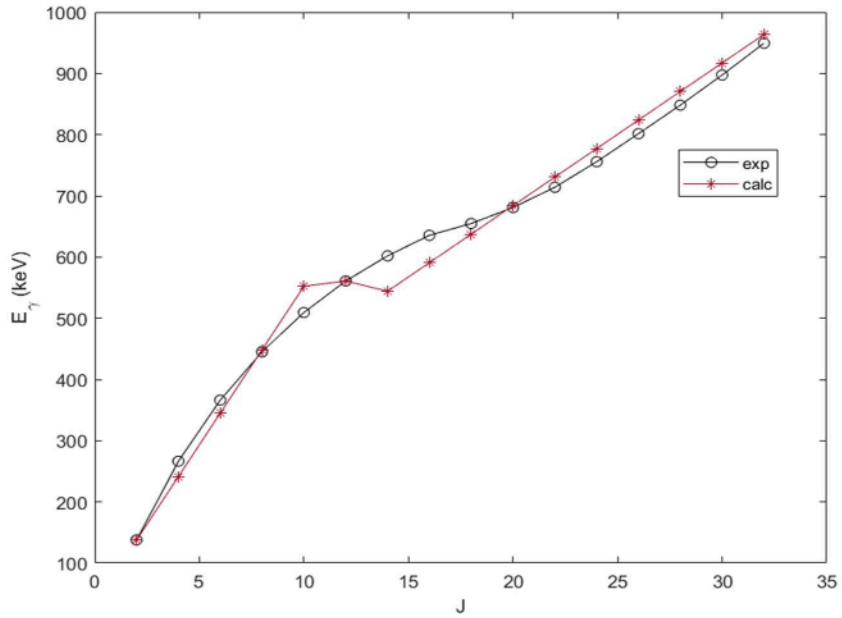

FIG. 7. Transition energy (E_γ) changes with momentum (J).

Gama transitions and their probabilities between different energy levels are important parameters in the study of the nuclear properties of any isotope. We calculated this function, B(E2), for different transitions between multiple levels of the isotope under study and compared it with the experimental results. This calculation was based on available laboratory values for the gamma energies of different transitions, the half-life of the gamma transition, and the available values for the isotope internal transformation coefficient. Using Eq. (10), we determined the electric transition probabilities of the quadrupole, B(E2). Table 7 shows that the results are in good agreement with the experimental values.

TABLE 7. Electromagnetic transitions using the half-life of the $^{156}_{66}Dy$ isotope.

I^π	$T_{\frac{1}{2}(exp)}(ps)$	$E_\gamma(KeV)$	$\propto^+_{tot}$	B(E2) W.u		error
				exp	clc	
$2^+ \rightarrow 0^+$	823	137.77	0.849	150	150.07	0.049
$4^+ \rightarrow 2^+$	31.6	266.42	0.0933	244.8	244.43	0.151
$6^+ \rightarrow 4^+$	6.3	366.25	0.0356	264	263.63	0.140
$8^+ \rightarrow 6^+$	2.26	445.17	0.0206	281	281.07	0.026
$10^+ \rightarrow 8^+$	1.06	509.41	0.01444	310	307.29	0.875
$12^+ \rightarrow 10^+$	0.62	560.86	0.01131	330	325.74	1.292
$14^+ \rightarrow 12^+$	0.56	601.94	0.0095	250	253.72	1.488
$16^+ \rightarrow 14^+$	0.32	635.48	0.00833	340	338.96	0.305
$18^+ \rightarrow 16^+$	0.24	654.8	0.00776	390	389.32	0.175
$20^+ \rightarrow 18^+$	0.24	680.9	0.0708	320	320.42	0.132
$22^+ \rightarrow 20^+$	0.21	714	0.00634	290	289.04	0.331
$24^+ \rightarrow 22^+$	0.155	755.7	0.00557	300	295.07	1.644

Fig. 8 shows the relationship between the ratio $r\left(\frac{(I+2)}{I}\right)$ and the spin I. This figure provides numerical values for this ratio. It is clear that the ratio was between $0.4 \leq r \leq 0.6$ for the spin higher than 6, so we can say that the Dy (156) isotope has γ-unstable properties with the O(6) limit. However, for the lower spins of 2, 4, and 6 these ratios reached up to 0.7, so the nuclei could have rotating properties. Despite this, most of the given spin ranges were found within the O(6) limit. Table 8 shows the typical ratio value (r) for each limit.

TABLE 8. Typical values for ratios.

Symmetry	$r\left(\frac{(I+2)}{I}\right)$
U (5)	$0.1 \leq r \leq 0.35$
O (6)	$0.4 \leq r \leq 0.6$
SU (3)	$0.6 \leq r \leq 1$

Fig. 9 shows the staggering between the energy states of the GSB and NPB bands in the Dy (156) isotope. This staggering is evidence of the interference of the energy states between the two bands.

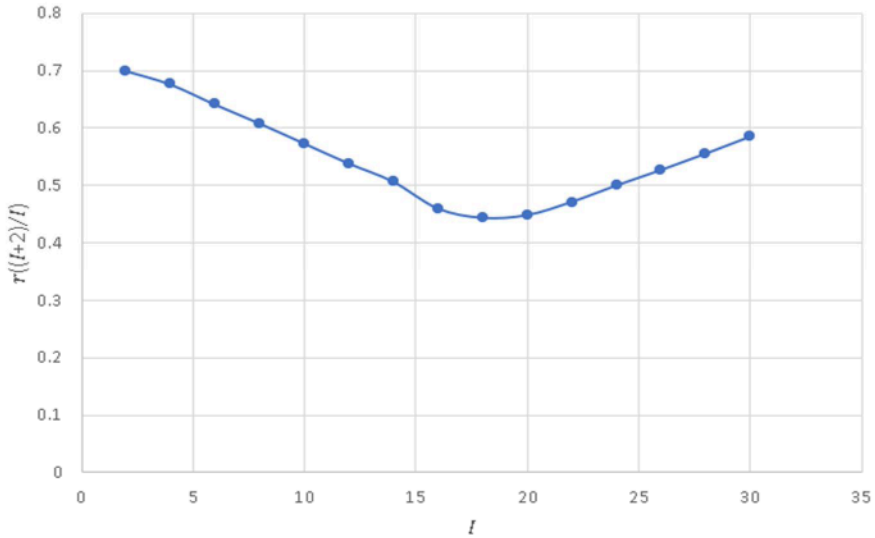

FIG. 8. The ratio between any two consecutive states in the beam.

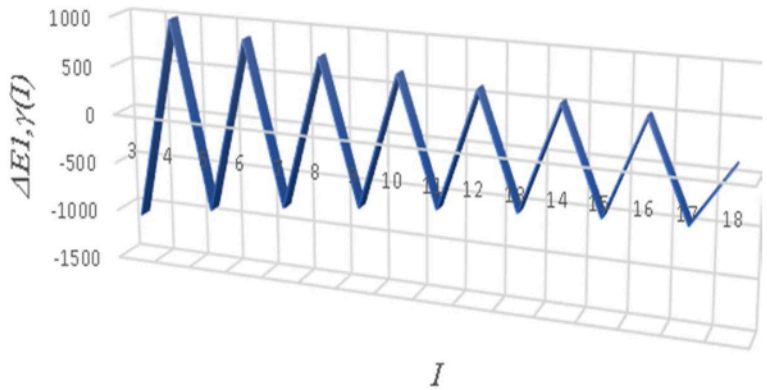

FIG. 9. Staggering patterns between GSB and NPB.

Conclusion

In this work, we carried out a systematic investigation of the even-even $^{156}_{66}Dy$ isotope within the IBM-1 and IVBM frameworks. We calculated the yrast and negative band energy levels. The ratio values ($E(I+2)/E_2^+$), ($E(I+2)/E(I)$), and $r\left(\frac{(I+2)}{I}\right)$ indicate that this isotope is due to the γ - unstable symmetry. Additionally, the calculated moment of inertia and $\hbar\omega$ values show good agreement with experimental data. In this isotope, the back-bending phenomenon does not appear clearly at J =10, but there is a slight change in the track of the curve of the relationship between photon energy and moment of inertia in the interval $10 \geq J \geq 20$.

References

[1] Safauldeen, O.A. and Shatti, W.A., Diyala J. Pure Sci., 14 (2018) 1.

[2] Arima, A. and Iachello, F., Phys. Lett. B, 53 (1974) 309.

[3] Hasan, M., Tabussum, M., Roy, P. et al., Res. Trends Challenges Phys. Sci., 7 (2022) 1.

[4] Abood, S.N. and Najim, L.A., Int. J. of Phys., 4 (2016) 1.

[5] Alnejm, M.A.A., Kirkuk Univ. J. Sci. Stud. (KUJSS), 16 (2021) 1.

[6] Arias, J.M., Dukelsky, J., et al., Phys. Rev., C, 75 (2007) 014301.

[7] Al-Khudair, F.H., Long, G.L., and Sun, Y., Phys. Rev., 77 (2008) 034303.

[8] Nasef, D. et al., The Fourth Int. Conf. Sci. Tech., 20 (2021) 4.

[9] Georgieva, A., Raychev, P., and Raussev, R., J. Phys. G, Nucl. Phys., 8 (1982) 1377.

[10] Ganev, H., Garistov, V.P., and Georgieva, A.I., Phys. Rev. C, 69 (2004) 014305.

[11] Ganev, H. et al., Phys. Rev. C, 70 (2004) 054317.

[12] Georgieva, A., Raychev, P., and Roussev, R., Bulg. J. Phys., 12 (1983) 147/ J. Phys. G, 9 (1985) 521.

[13] Georgieva, A. and Garistov, V.P., J. Phys.: Conf. Ser., 590 (2015) 012033.

[14] Khalaf, A.M., Ahmed, G.S.M. et al., Nuclear Physics A, 988 (2019) 1-8.

[15] Ganev, H., Garistov, V.P., and Georgieva, A.I., Institute of Nuclear Research and Nuclear Energy, 1 (2003) 25.

[16] Giannatiempo, A., Phys. Rev. C, 84 (2011) 024308.

[17] Nasef, D. et al., Sebha University J. Pure Appl. Sci., 20 (2021) 2.

[18] Abood, S., Najim, L., and Jundy, Y., Int. J. Recent Res. Rev., VII (2014) 2.

[19] Bohr, A. and Mottelson, B.R., "Nuclear Structure", (Word Sci., Singapore, 1998), Vol. 2.

[20] Hossain, I., Sharrad, F. et al., Chiang Mai J. Sci., 42 (2015) 1.

[21] Meng, H., Hao, Y., et al., Prog. Theor. Exp. Phys., 103 (2018) D02.

[22] Liu, Y.X., Mu, L.-Z., and Wei, H.Q., Phys. Lett. B, 633 (2006) 49.

[23] Iachello, F. and Isacker, V.P., "The Interacting Boson-Fermion Model", (Cambridge University Press, 1991).

[24] Stephens, F.S. and Simon, R.S., Nucl. Phys. A, 183 (1972) 257.

[25] Yang, J., Hua-Lei, W., and Chai, Q., Prog. Theor. Exp. Phys., 063 (2016) D03.

[26] Satuła., W. and Wyss, R., Phys. Scripta T, 56 (1995) 159.

[27] Dieperink, A.E.L. and Wenes, G., Ann. Rev. Nucl. Part. Sci., 35 (1985) 1.

[28] Hossain, I. et al., J. Theo. App. Phys., 7 (2013) 46.

[29] Al-Jubboria, M. et al., Nucl. Phys. A, 971 (2018) 1.

[30] Casten, R.F. and Warner, D.D., Rev. Mod. Phys., 60 (1988) 389.

[31] Arima, A. and Iachello, F., Phys. Rev. lett., 35 (1975) 1069.

[32] Muaffaq, O.A. et al., Int. J. App. Eng. Res., 13 (2018) 11.

[33] Iachello, F., "Nuclear Structure", Eds. K. Abrahams, K. Allaart, and A.E.L. Dieperink (New York, Plenum Press, 1981).

[34] Islam, J. and Hossain, I., Prob. Atom. Sci. Tech., N5 (2016) 105.

[35] Iachello, F. and Arima, A., "The Interacting Boson Model. Cambridge Monographs on Mathematical Physics", (Cambridge University Press, 1987).

[36] Küçükbursa, A. et al., Math. Comput. Appl., 10 (2005) 1.

[37] Mutshera, S.M., Sharradb, F.I., and Salmand, E.A., Nucl. Phys. A, 1017 (2022) 1.

[38] Kassim, H.H. et al., 2nd Int. Sc. Conf. of Al-Ayen Univ., 928 (2020) 7.

[39] Regan, P.H., Beausang, C.W., Zamfir, N.V., et al., Phys. Rev. Lett., 90 (2003) 152502.

[40] Eshaftri, N.S. et al., Libyan J. Sci., 24 (2021) 1.

[41] Mutsher, S.M., Salman, E.A. and Sharrad, F.I., 2nd Int. Sc. Conf. of Al-Ayen Univ., 928 (2020) 7

[42] Ahmed, I.M. and Al-Jabbori, M.A., J. Rafidain Sci., 20 (2009) 4.

[43] Georgieva, A. et al., Phys. Part. Nucl., 40 (2009) 4.

[44] Ganev, H.G., Bulgarian J. Phys., 48 (2021) 421.

[45] Arima, A. et al., Phys. Lett. B, 66 (3) (1977) 205.

[46] A-Jubbori, M.A., Kassim, H.H. et al., Phys. Atom. Nuclei., 82 (2019) 201.

[47] Ahmed, M.A. and Ahmed, I.M., J. Rafidain Sci., 28 (2019) 4.

[48] Johnson, A., Ryde, H., and Sztarkier, J., Phys. Lett. B, 34 (1971) 605

[49] Chapman, R. et al., Phys. Rev. Lett., 51 (1983) 2265.